# Journal Pre-proof


The fungal secretory peptide micasin induces itch by activating MRGPRX1/C11/A1 on peripheral neurons

Haifeng Yang, Yian Chen, Luyao Wang, Bing Gan, Leiye Yu, Ruobing Ren, Hang Fai Kwok, Yingliang Wu, Zhijian Cao

PII: S0022-202X(24)01871-2

DOI: https://doi.org/10.1016/j.jid.2024.05.031

Reference: JID 4369

To appear in: *The Journal of Investigative Dermatology*

Received Date: 5 December 2023

Revised Date: 3 May 2024

Accepted Date: 7 May 2024

Please cite this article as: Yang H, Chen Y, Wang L, Gan B, Yu L, Ren R, Kwok HF, Wu Y, Cao Z, The fungal secretory peptide micasin induces itch by activating MRGPRX1/C11/A1 on peripheral neurons, *The Journal of Investigative Dermatology* (2024), doi: https://doi.org/10.1016/j.jid.2024.05.031.

*Manuscript*

# The fungal secretory peptide micasin induces itch by activating MRGPRX1/C11/A1 on peripheral neurons

Haifeng Yang[1,2,§], Yian Chen[2,§], Luyao Wang[2], Bing Gan[3], Leiye Yu[3], Ruobing Ren[3], Hang Fai Kwok[4], Yingliang Wu[2], Zhijian Cao[1,¶]

[1] National "111" Center for Cellular Regulation and Molecular Pharmaceutics, Key Laboratory of Fermentation Engineering (Ministry of Education), Hubei University of Technology, Wuhan, China

[2] State Key Laboratory of Virology, College of Life Sciences, Shenzhen Research Institute, Wuhan University, Wuhan, China

[3] Shanghai Key Laboratory of Metabolic Remodeling and Health, Institute of Metabolism and Integrative Biology, Fudan University, Shanghai, China

[4] Department of Biomedical Sciences, Faculty of Health Sciences, University of Macau, Avenida de Universidade, Taipa, Macau SAR

§ These authors contributed equally to this work.

¶ Correspondence author: Zhijian Cao (National "111" Center for Cellular Regulation and Molecular Pharmaceutics, Key Laboratory of Fermentation Engineering, Hubei University of Technology, Wuhan, China. E-mail: 20241002@hbut.edu.cn).

## ORCiDs

Haifeng Yang: https://orcid.org/0009-0001-1229-4347

Yian Chen: https://orcid.org/0009-0005-5681-1210

Luyao Wang: https://orcid.org/0000-0002-9976-5438

Bing Gan: https://orcid.org/0000-0002-2226-3165

Leiye Yu: https://orcid.org/0000-0001-8698-6787

Ruobing Ren: https://orcid.org/0000-0003-4517-7216

Hang Fai Kwok: https://orcid.org/0000-0002-6349-4517

Yingliang Wu: https://orcid.org/0000-0002-7204-6484

Zhijian Cao: https://orcid.org/0000-0002-2603-5434

## Abstract

Pruritus is the leading symptom of dermatophytosis. *Microsporium canis* is one of the predominant dermatophytes causing dermatophytosis. However, the pruritogenic agents and the related molecular mechanisms of the dermatophyte *M. canis* remain poorly understood. Here, the secretion of the dermatophyte *M. canis* was found to dose-dependently evoke itch in mice. The fungal peptide micasin secreted from *M. canis* was then identified to elicit mouse significant scratching and itching responses. The peptide micasin was further revealed to directly activate mouse dorsal root ganglia (DRG) neurons to mediate the non-histaminergic itch. Knockout and antagonistic experiments demonstrated that MRGPRX1/C11/A1 rather than MRGPRX2/b2 activated by micasin contributed to pruritus. The chimera and mutation of MRGPRX1 showed that three domains (ECL3, TMH3 and TMH6) and four hydrophobic residues (Y99, F237, L240 and W241) of MRGPRX1 played the key role in micasin-triggered MRGPRX1 activation. Our study sheds light on the dermatophytosis-associated pruritus and may provide potential therapeutic targets and strategies against pruritus caused by dermatophytes.



## Key words

Dermatophytosis; *Microsporium canis*; Fungal defensin; Itch; Mrgprs

## Introduction

Dermatophytosis is an infection of the skin and subcutaneous keratinous tissue caused by a group of filamentous fungi known as dermatophytes (Cole et al., 2017). It has the highest prevalence of any infectious skin disease and affects more than 20 to 25% of the global population (Zhan and Liu, 2016). Infections caused by dermatophytes are a global problem and a major public health burden worldwide today (Gnat et al., 2021). *Microsporium canis* is one of the main clinical dermatophytes and has been found to be the leading pathogen causing tinea capitis and tinea corporis in various countries (Chen et al., 2021, Kromer et al., 2021, Moskaluk and VandeWoude, 2022). The zoonotic infection of *M. canis* with cats and dogs as leading reservoirs is commonly triggered by close contact between human and sick animals, or healthy carriers (Moriello et al., 2017, Moskaluk and VandeWoude, 2022). Scaling alopecia with inflammation or scaly erythema on the trunk are typical clinical signs in the infections mostly caused by *M. canis.* Severe pruritus is also commonly accompanied by the above symptoms (Dhaille et al., 2019, Suzuki et al., 2023, Yang et al., 2021, Zhi et al., 2021). However, the pruritogenic agents remain poorly understood during the infection of the dermatophyte *M. canis*.

Itch is an unpleasant sensation that caused people to scratch and has been evolved as an alarm aiming to remove irritants on the skin. It is considered as a self-protection mechanism to human (Dong and Dong, 2018). The itch pathway in the peripheral nervous system is divided into histaminergic itch and non-histaminergic itch (Lay and Dong, 2020). Classical histamine-dependent itch is mediated by cross-linking of allergen and IgE antibody binding to FcεRI receptor on mast cells. This cross-linking causes mast cells to degranulate and release histamine, which activates histamine receptor 1 (H1R) and histamine receptor 4 (H4R) on the dorsal root ganglia (DRG) to elicit itch (Simons and Simons, 2011). Mas-related G protein–coupled receptors (MRGPRs), a large family of GPCRs mainly expressing on small diameter nociceptive neurons and mast cells, play an important role in non-histaminergic itch (Cevikbas and Lerner, 2020). There are 27 members of the MRGPR family in mice, 13 in rats and 8

in human excluding pseudogenes, all of which are divided into nine subfamilies based on their sequence similarities: MRGPRA-H and X. The MRGPRA, B, C and H subfamilies are endemic in rodents, MRGPRD, E, F and G subfamilies are present in both rodents and primates, and MRGPRX is the primate-specific subfamily (Bader et al., 2014). Four members of human MRGPRX subfamily, MRGPRX1-X4, selectively activated by various pruritogens elucidate the reasons for some pruritus and inflammations that cannot be relieved by antihistaminic drugs (Al Hamwi et al., 2022). Human MRGPRX1 is responsible for scratching induced by chloroquine, bovine adrenal medulla peptide 8-22 (BAM8-22), cysteine protease (Liu et al., 2009, Reddy et al., 2015, Wilson et al., 2011). Human MRGPRX2 expressed in mast cell responds to a variety of cationic drugs which account for pseudo-allergic drug reactions (McNeil et al., 2015, Wolf et al., 2021). Human MRGPRX4 activated by bilirubin and bile acids contributes to cholestatic pruritus (Meixiong et al., 2019b, Meixiong et al., 2019c). It is not clear which class of itch and receptor are involved in pruritus caused by the dermatophyte *M. canis* and even other dermatophytes.

In our study, the fungal secretion from *M. canis* was firstly found to induce the itchy effect in mice. The dermatophytic secretory peptide micasin from *M. canis* was then identified to cause the scratching behavior in mice. We further found that the peptide micasin directly activated mouse wild-type DRG neurons and MRGPRX1/C11/A1 or MRGPRX2/b2-overexpressed HEK293T cells. Next, the experiments of gene editing mice (*MrgprC11*$^{-/-}$ and *Mrgprb2*$^{-/-}$) and specific antagonist demonstrated that MRGPRX1/C11/A1 rather than MRGPRX2/b2 mediated the histamine-independent itch induced by the fungal secretory peptide micasin. Finally, we used MRGPRX1-MRGPRX3 chimeras and alanine mutations to identify the key domains and residues of MRGPRX1 responding to the peptide micasin. The current work elucidates the pruritogenic component and its molecular mechanism of itch caused by the infection of *M. canis* and may provide potential therapeutic targets and strategies against itch in dermatophytosis.

## Results

### The fungal secretion of the dermatophyte *M. canis* evoked itch in mice.

Many fungal pathogenic factors were previously found to exist in the form of secreted proteins (Bi et al., 2023, Wang et al., 2014), and so the fungal secretion of *M. canis* was first obtained to investigate the pruritogenic agent of itch caused by the dermatophyte. The *M. canis* (ATCC 10214) was cultured on SDA plates and formed the phenotype of white downy-type colonies with radial grooves after two weeks (Figure 1a). The mycelium and spores of *M. canis* were gathered in 0.05% Tween-80 and subjected to slight ultrasonic treatment to release the fungal secretions on the cell wall. The supernatant containing fungal secretions was collected and purified by RP-HPLC. The peak of 0-6 min was considered as the component of salt in the supernatant and the peak of 7-30 min was collected for desalination (Figure 1b). Subsequently, intradermal injection of the desalinated secretion at different doses elicited significant scratching behavior in mice, which hinted the presence of pruritogen in the fungal secretion from *M. canis* (Figure 1c). The peaks of three time periods (7-12 min, 13-20 min and 21-30 min) in the demineralized fungal secretion were further collected to determine the retention time of the pruritogenic mediator by RP-HPLC (Figure 1d). Compared to the collections of two time periods (7-12 min and 21-30 min), the collective component in the 13-20 min period only evoked pruritus in mice (Figure 1e). Furthermore, the fungal secretory component at the retention of 13-20 min dose-dependently triggered scratching behavior in mice (Figure 1f). These results indicate that the fungal secretions of *M. canis* have pruritogens and are well associated with pruritus in the infection of the dermatophyte *M. canis.*

### The fungal secretory peptide micasin from *M. canis* elicited itch in mice.

To investigate the detailed pruritogens in the fungal secretion, the secretory components of the dermatophyte *M. canis* were detected by LC-MS/MS. The top 10 components of Sum PEP Score in the mass spectrometry result included glycoproteins

of fungal cell walls (extensin and tenascin C), stress proteins (hsp70-like protein, antioxidant protein LsfA, stress protein DDR48 and Cu/Zn superoxide dismutase), fungal defensin (micasin) and three conserved hypothetical proteins (Figure 2a). Micasin in the fourth place on Sum PEP Score, a peptide identified from *M. canis* caught our attention with a sequence coverage of 100% (Figure 2a). The N-terminus and C-terminus of the peptide identified by mass spectrometry could be spliced into the complete peptide micasin and showed the high protein abundance (Figure 2b-d). Interestingly, the peptide micasin was a dermatophytic defensin with potent antibacterial activity (Zhu et al., 2012), and tick defensins and mouse/human β-defensins were recently found to induce itch (Li et al., 2021, Tseng and Hoon, 2022, Zhang and McNeil, 2019). So, we inferred that the peptide micasin might evoke pruritus in mice. To investigate the itch effect of the peptide, the reduced micasin (Micasin-Re) with a purity of more than 95% was chemically synthesized and then it was folded by one-step air oxidation in 0.1 M Tris HCl buffer (pH 8.5, 28 °C). The oxidized micasin (Micasin-Ox) with earlier retention time than Micasin-Re was purified via RP-HPLC (Figure 2e). Furthermore, the molecular mass of the oxidized product determined by MALDI-TOF/MS was 4055.44 Da, which was 6 Da less than that of Micasin-Re because of the formation of 3 disulfide bridges (Figure 2e). Micasin-Ox also exhibited a cysteine-stabilized α-helical and β-sheet (CSαβ) fold compared to Micasin-Re in the circular dichroism (CD) spectra analysis (Figure 2f). These results showed that Micasin-Ox was successfully prepared *in vitro*. Subsequently, the itchy effect of the peptide micasin was investigated. Micasin-Ox evoked a significant itchy behavior in a dose-dependent manner in mice compared to saline and Micasin-Re in the nape model (Figure 2g). Micasin-Ox also did not elicit pain behaviors (wipping) in the cheek model, indicating the exclusive itch effect caused by the peptide micasin (Supplementary Figure S1). All these results shows that the peptide component micasin of the fungal secretion from *M. canis* evokes itch in mice, dependent on the formation of disulfide bridges and fold.

**Micasin triggered non-histaminergic itch by directly activating DRG in mice.**

Histaminergic and non-histaminergic itch were the two main pathways in the peripheral itch. Classic histamine-dependent itch was mediated by the mast cell degranulation. The degranulation of mast cells releases all kind of substances including histamine, serotonin, tryptase beta 2, and so on. The released components target different cells and then induce diverse functions. For example, the released histamine from mast cells activates the membrane receptors H1R and H4R on DRG neurons to evoke itch. And so, itch ligands could not directly activate itch-sensing neurons in the histaminergic itch pathway. On the contrary, the ligands of non-histaminergic itch could directly activate DRG neurons by targeting the related itchy receptors. At the same time, our group and Zhang et al. reported that tick defensins and mouse β-defensins activated MRGPRs receptors on itch-sensing neurons (Li et al., 2021, Zhang and McNeil, 2019). In view of the above, we investigated whether the fungal secretory defensin peptide micasin activated DRG neurons in mice. Resultedly, Micasin-Ox induced intracellular calcium influx in DRG neurons isolated from mice, which showed the peptide micasin could directly act on primary sensory neurons (Figure 3a; Supplementary Figure S2). The direct activation of DRGs evoked by Micasin-Ox suggested that the pruritus caused by the peptide might be non-histaminergic itch pathway. To further confirm whether histamine was involved in itch caused by Micasin-Ox, two histamine receptor antagonists were used. Consistent with our speculation, the treatment with CETY (a histamine receptor H1 antagonist) and JNJ7777120 (a histamine receptor H4 antagonist) dramatically also relieved histamine-induced scratching responses but failed to reduce scratching behavior induced by Micasin-Ox (Figure 3b), which showed that the peptide micasin was involved in the histamine-independent itch caused by the secretions. These results show the peptide micasin induces non-histaminergic itch by directly activating DRG in mice.

**MRGPRX1/C11/A1 mainly mediated histamine-independent itch induced by micasin.**

MRGPRs, protease-activated receptors (PARs) and cytokine receptors were the three main receptor families that mediated non-histamine dependent itch. Interestingly, the tick defensin IPDef1 evoking itch by activating MRGPRX1/C11, shared a high amino acid sequence similarity to micasin. So, we inferred that micasin-induced itch was an Mrgpr-dependent neural pathway and then examined the activation effect of the fungal peptide on MRGPRX1/C11 by live cell calcium imaging. Human MRGPRX1 (hMRGPRX1) and its ortholog mouse MrgprC11 (mMrgprC11) were both strongly activated by Micasin-Ox (Supplementary Figure S3a-b). The dose-response curves for hMRGPRX1 and mMrgprC11 expressed in HEK293T cells to Micasin-Ox figured out that $EC_{50}$ values of Micasin-Ox were 2.75 μM and 1.71 μM, respectively (Figure 3c). The activation effect of Micasin-Ox on other mouse Mrgprs also were further investigated. Interestingly, Micasin-Ox did not respond to the other mouse ortholog receptor MrgprA3 ($EC_{50}$=n.d.) of human MRGPRX1. However, MrgprA1 was appropriately activated by Micasin-Ox ($EC_{50}$=9.69 μM). Other mMrgprs (Mrgpra2b, MrgprB4, B5, D, E) failed to be activated by Micasin-Ox (Figure 3c; Supplementary Figure S3c-i).

In addition to HEK293T cells overexpressing Mrgprs, we also compared the activation effect of Micasin-Ox on different Mrgprs in mouse DRG neurons by various Mrgpr agonists stimulating the same cells (Supplementary Figure S4). Among 4333 KCl-responsive neurons, the number of neurons activated by Micasin-Ox was 155 (3.6%, Micasin/KCl), BAM8-22 (MrgprC11 agonist) was 221 (5.1%, BAM/KCl), CQ (MrgprA3 agonist) was 151 (3.48%, CQ/KCl) and FMRF (MrgprA1 agonist) was 147 (3.4%, FMRF/KCl). Micasin and BAM8-22 co-responsive neurons number was 96 (62%, co-re/Micasin). Micasin and CQ co-responsive neurons number was 32 (20.6%, co-re/Micasin). Micasin and FMRF co-responsive neurons number was 72 (46.5%, co-re/Micasin) (Supplementary Figure S5). Among 365 four ligand-responsive neurons, the number of neurons that co-respond to Micasin-Ox and BAM8-22 but did not react to CQ and FMRF was 44 (12%), co-respond to Micasin-Ox and FMRF but did not react to BAM8-22 and CQ was 25 (6.8%), co-respond to Micasin-Ox and CQ but did not

react to BAM8-22 and FMRF was only 2 (0.5%) (Figure 3d). The results suggested that Micasin-Ox preferred to activate BAM8-22-responsive neurons and FMRF-responsive neurons, rather than CQ-responsive neurons.

To further investigate the role that mMrgprC11/A1 plays in micasin-induced itch, we firstly compared micasin-evoked $Ca^{2+}$ signals in DRG neurons isolated from MrgprC11-deficient mice with those isolated from wild-type (WT) littermates and found that the $Ca^{2+}$ signals evoked by micasin were significantly attenuated in MrgprC11-deficient DRG neurons as well as the control BAM (Supplementary Figure S6). The cultured DRG neurons isolated from MrgprC11-deficient mice showed a decrease in the proportion of micasin-sensitive neurons compared with that among WT mouse DRG neurons (Figure 3e). Moreover, the gene deletion of MrgprC11 in mice did not affect the expression of other Mrgprs (Supplementary Figure S7). We also evaluated the itching responses induced by micasin in MrgprC11-knockout mice. As expected, the scratching responses induced by micasin were dramatically decreased in MrgprC11-deficient mice compared with WT mice (Figure 3f). These results suggest that MrgprC11 plays a key role in itch mediated by micasin.

Next, MrgprA1 inhibitor QWF (Azimi et al., 2016) was used to explore whether MrgprA1 was involved in pruritus induced by Micasin-Ox in mice. At the same time, MrgprA3 inhibitor Berbamine (BBM) (Ryu et al., 2022) was also used as the system control. Pruritus caused by CQ rather than Micasin-Ox in mice was reduced by BBM (Figure 3g) and QWF slightly alleviated scratching behaviors elicited by Micasin-Ox and bilirubin (Figure 3h), which manifested that MrgprA1 instead of MrgprA3 to some extent contributed to itch evoked by micasin. In summary, all results show that MRGPRX1/C11 is the main receptor mediating itch caused by the peptide micasin and MrgprA1 is partially involved in the pruritus.

**Activation of MRGPRX2/b2 by micasin triggered inflammation rather than itch.**

The peptide micasin was also found to moderately activate the itch receptor of human MRGPRX2 and its ortholog mouse Mrgprb2 (Figure 4a and b) but had no effects on

both human MRGPRX3 and human MRGPRX4 (Supplementary Figure S8). The MRGPRX2 and Mrgprb2 expressed on mast cell contributed to acute inflammation and pseudoallergy. But some previous reports also showed that mast cell activation by Mrgprb2 evoked itch in mice (Meixiong et al., 2019a). So, we prepared Mrgprb2 knockout mice to further investigate the role of MRGPRX2/b2 in pruritus induced by Micasin-Ox (Supplementary Figure S9*)*. The *in vivo* results showed that the scratching responses induced by Micasin-Ox had no obvious difference between Mrgprb2 knockout mice and WT mice, but the pruritus caused by PAMP9-20 was attenuated in Mrgprb2 knockout mice. The result demonstrated that Mrgprb2 was not involved in the itch evoked by Micasin-Ox (Figure 4c). Moreover, sodium cromoglycate, a classic mast cell degranulation inhibitor, also did not affect itch caused by Micasin-Ox (Figure 4d), which suggested that mast cells were not related to trigger scratching caused by the peptide micasin in mice. We inferred that the main function of Mrgprb2 activated by Micasin-Ox may mediate inflammation. The evans blue experiment was used to measure the extent of inflammation by the analysis of extravasation upon injection of the peptide into the footpad. In agreement with our speculation, the peptide micasin caused extensive extravasation at different doses (Figure 4e). The extravasation caused by Micasin-Ox was greatly alleviated in Mrgprb2 knockout mice, a level that was not statistically different from saline injection (Figure 4f). Anti-IgE that mediated degranulation of mast cells by activating FcεRI receptor was not affected by the knockout of Mrgprb2. By contrast, compound 48/80, an agonist of Mrgprb2, showed minimal extravasation in Mrgprb2 knockout mice compared to wild type mice (Figure 4f and g). These results suggest that MRGPRX2/b2 is involved in inflammation instead of itch caused by the fungal secretory peptide micasin.

**Three domains and four residues of MRGPRX1 are critical in the micasin-triggered MRGPRX1 activation.**

The amino acid sequence similarity between MRGPRX1 and MRGPRX3 was 90.79% (Figure 5a), but the peptide micasin only showed the potent activation to MRGPRX1

rather than MRGPRX3, which suggested the different amino acids between MRGPRX1 and MRGPRX3 had a significant impact on the activation of Micasin-Ox to MRGPRX1. MRGPRs belonging to G protein-coupled receptors families can be divided into N-terminal, C-terminal, three extracellular loops (ECL1-3), seven transmembrane helical domain (TMH1-7) and three intracellular loops (ICL1-3) in topological structure. Except for ICL1 and TMH7, the other structural domains of MRGPRX1 are different from those of MRGPRX3 (Figure 5b). Our group recently constructed the MRGPRX1(X3-domain) chimeras that replaced the domain of MRGPRX1 with the corresponding MRGPRX3 domain to identify key domains and residues of MRGPRX1 recognizing BAM8-22 (Hu et al., 2023). Such strategy was also used to identify key domains and residues of MRGPRX1 binding the peptide micasin (Figure 5b). The activation effect of Micasin-Ox on thirteen chimeras transfected into HEK293T cells were detected by calcium imaging. Three chimeras MRGPRX1(X3-ECL3), MRGPRX1(X3-TMH3) and MRGPRX1(X3-TMH6) failed to respond to Micasin-Ox, but other ten chimeras were normally activated by the peptide (Figure 5c-e; Supplementary Figure S10). These results show that the different amino acids in the three domains (ECL3, TMH3 and TMH6) between MRGPRX1 and MRGPRX3 play a crucial role in recognizing the peptide micasin. To further investigate key residues of MRGPRX1 activated by Micasin-Ox, plasmids with the single point mutation on the differential amino acid in the three domains were constructed (Figure 5f). Four mutations of TMH3 Y99S, TMH6 F237A, ECL3 L240S and W241R failed to be activated by Micasin-Ox (Figure 5g-j). But other nine mutations showed normal activation effects (Supplementary Figure S11). All these results indicate that three domains (ECL3, TMH3 and TMH6) and four hydrophobic residues (Y99, F237, L240 and W241) play critical roles in the activation of MRGPRX1 evoked by the fungal secretory peptide micasin.

## Discussion

An increased prevalence of superficial fungal infections caused by dermatophytes has been observed worldwide (Chanyachailert et al., 2023, Martinez-Rossi et al., 2021). At present, approximately 40 kinds of dermatophytes are found to cause pathogenic effects on humans, and these pathogens can be mainly divided according to their usual habitat into: anthropophilic, zoophilic and geophilic organisms (Segal and Elad, 2021). Zoophilic dermatophytes are found in animals, which were one of the main pathogens causing tinea capitis. Source of the zoophilic infection were small household pets, such as cats, dogs, guinea pigs and rodents. Human may suffer from ringworm by direct contact with sick animals and healthy carriers (Chermette et al., 2008). With the popularity of family pets, more people are enjoying intimate interactions with their companion animals, and the risk of the zoophilic dermatophyte infection is also increasing (Paryuni et al., 2020). In the background, *M. canis* with cats and dogs as leading reservoirs has been currently the most prevalent zoophilic dermatophyte worldwide (Chen and Yu, 2023). The infections caused by *M. canis* with intense inflammation and pruritus brings enormous burdens to patients. However, the mechanisms behind pruritus caused by *M. canis* and even other dermatophytes was still unclear.

In our study, we firstly found that the fungal secretion of *M.canis* significantly induced itching and scratching responses in mice. Subsequently, the peptide micasin from the fungal secretion was identified to evoke pruritus in mice by non-histamine dependent pathway. Interestingly, some studies reported that histamine may be involved in pruritus caused by dermatophytes. Immediate hypersensitivity could be elicited by several allergens (*Tri t* 1, *Tri t* 4 and *Tri r* 2) from the genus *Trichophyton.* The intense itch associated with elevated histidine decarboxylase (HDC) expression in a contact dermatitis mouse model induced by trichophytin, a crude extract from *T. mentagrophytes* was also observed (Lund and DeBoer, 2008, Nakamura et al., 2018, Woodfolk et al., 2000). On the other hand, pruritus elicited by the dermatophyte *Arthroderma vanbreuseghemii* (ADV) extract was mediated by the non-histaminergic pathway rather than the histaminergic pathway. The ADV extract with the activity of

serine protease led to itching through protease-activated receptor 2 (PAR2) in mice, which was reasonable owing to that numerous proteases were secreted by dermatophytes to digest keratin (Andoh et al., 2012, Descamps et al., 2002). These results suggested that the complex itch mechanism of dermatophytes, where different pruritogens induced pruritus by different signal pathways.

Secondly, the peptide micasin could mediate cellular calcium influx by activating hMRGPRX1, hMRGPRX2 and their mouse orthologs (mMrgprC11 and mMrgprb2). This result was interesting, but not unexpected. In 1966, defensins were first discovered to be a class of lysosomal cationic peptides with antibacterial activity in polymorphonuclear leukocytes (Zeya and Spitznagel, 1966). Natural defensins were then found to be distributed in almost all biological groups from actinomycetes, fungi, plants, and lower animals to mammals (Lima et al., 2022, Ng et al., 2013, Selsted and Ouellette, 2005, Zhu et al., 2022). Defensins not only have retained antimicrobial activity throughout evolution, but also plays crucial roles in inflammation, itch and immunomodulation (Cosi and Gadermaier, 2023, Guryanova and Ovchinnikova, 2022). Subramanian et al. firstly found that hBD2 (Human β-defensin 2) and hBD3 (Human β-defensin 3) could activate human mast cells through MRGPRX2 in 2013 (Subramanian et al., 2013). Similarly, RC-100 (a humanized θ-defensin) and PG-1 (a θ-defensin-like peptide isolated from porcine leukocytes) could cause calcium mobilization and degranulation in rat basophilic leukemia (RBL-2H3) cells stably expressing MRGPRX2 (Gupta et al., 2015). In 2019, Zhang et al. reported that mouse defensins Defb3 and Defb14 could activate not only MRGPRX1 or MrgprC11 but also Mrgprb2 to mediate acute vascular permeability (Zhang and McNeil, 2019). Human defensins (DEFB4 and DEFB103) and tick-defensin IPDef1 were also recently found to activate both MRGPRX1 and MRGPRX2, respectively reported by Hoon group and our group (Li et al., 2021, Tseng and Hoon, 2022). These studies showed that defensins evoked mast cell degranulation to mediate inflammatory responses by activating MRGPRX2/b2. But the releasing substances (like histamine and trypsase) from mast cells by degranulation would activate the related itchy receptors on DRGs and then

induce scratching behavior. It was not clear whether the activated pathway (Defensin-MRGPRX2/b2) was involved in pruritus caused by defensins. MrgprC11-knockout and Mrgprb2-knockout mice constructed by our group successfully solved the problem. The peptide micasin showed stronger activation effects on MRGPRX1/C11, compared to MRGPRX2/b2. MrgprC11-knockout and Mrgprb2-knockout mice further confirmed that the peptide micasin induced itch by MrgprC11 rather than Mrgprb2. On the contrary, the activation of Mrgprb2 caused by micasin led to the acute inflammation, which might also be one of the reasons for clinical symptoms of redness and swelling caused by the infection of *M. canis.*

Although various defensins exhibited conserved activation effect on human MRGPRX1 and X2, diversity of sensitization to mouse Mrgprs orthologs are increasingly found. Tick defensin IP-O sharing 63.15% amino acid sequence similarity with micasin responded to MrgprA3 instead of MrgprA1. But the peptide micasin unexpectedly activated MrgprA1 rather than MrgprA3 in the study. Interestingly, mouse β-defensin Defb14 showed strong activation effects on MRGPRX1 ($EC_{50}$=0.61 μM), MrgprA1 ($EC_{50}$=0.62 μM) and MrgprA3 ($EC_{50}$=1 μM) but low response to MrgprC11 ($EC_{50}$=21.6 μM) (Tseng and Hoon, 2022). These results revealed that non-conserved amino acids of defensins may determine the selectivity of defensins to Mrgprs.

Thirdly, key domains and residues of MRGPRX1 recognizing micasin were identified by MRGPRX1(X3-domain) chimeras and mutations. The amino acid sequence similarity between MRGPRX1 and MRGPRX3 was extremely high (90.79%), but the peptide micasin could only activate MRGPRX1 rather than MRGPRX3. Our results showed that the mutated MRGPRX1 with Y99S of THM3, F237A of TMH6, and L240S and W241R of ECL3 could not be activated by the peptide micasin, which suggested that the difference of hydrophobicity and hydrophilicity in binding pocket between MRGPRX1 and MRGPRX3 ligands led to receptor selectivity. MRGPRX3 had a hydrophilic ligand pocket (S99, A237, S240 and R241). On the contrary, the pocket of MRGPRX1 was hydrophobic (Y99, F237, L240 and W241), which was observed by three different groups resolving the cryo-EM complex structures of

MRGPRX1 and ligands (Gan et al., 2023, Guo et al., 2023, Liu et al., 2023).

Finally, there are still some unresolved issues in this study. The necessity and sufficiency of micasin in dermatophytosis-associated itch is not assessed in our study. To elucidate this issue, there are three points that need to be addressed. Firstly, the *M. canis* mutant strains lacking micasin gene need to be generated. Secondly, an *in vivo* animal model of dermatophytosis infection need to be established. Thirdly, a set of methods for assessing the degree of itch in the model need to be developed.

In summary, our work characterizes and identifies, to our knowledge, a previously unreported pruritogen, the fungal secretory peptide micasin from the dermatophyte *M. canis,* evoking dermatophytosis-related itch by activating MRGPRX1/C11/A1 in pruriceptors, which will possibly provide potential therapeutic targets and strategies against itch in dermatophytosis.

## Materials and Methods

### Identification and cultivation of the fungal strain

The *M. canis* (ATCC 10214) was purchased from the Mingzhou Biotechnology Co., Ltd. The strain was then transferred to Sabouraud Dextrose Agar (SDA) plate at 28 °C for two weeks. The fungi were scraped from the plate using a sterilized scraper, put into mortar, and fully grinded with liquid nitrogen. Genomic DNA were extracted using Fungal Genomic DNA Isolation Kit (Sangon Biotech, Shanghai, China). Ribosomal internal transcribed spacer (ITS) sequences were used to identify the clinical strain (Supplementary Figure S12). The primers for amplifying internal transcribed spacer (ITS) region of nuclear ribosomal DNA were ITS-FP (5'-TCCGTAGGTGAACCTGCGG-3') and ITS-RP (5'-TCCTCCGCTTATTGATATGC-3').

### Extraction and identification of fungal secretion

The mature spores and hyphaes that had grown in SDA plate at 28 °C for two weeks

were collected in 0.05% Tween-80. Then the collected fungi were subjected to slight ultrasonic treatment (40 kHz) in ice water for ten minutes to release secretions on the cell wall. The supernatant of fungi that was obtained by centrifuge (12000 g, 15 min, 4 °C) was further purified by reversed phase-high performance liquid chromatography (RP-HPLC). The peak of the supernatant in different periods was collected and freeze-dried into the solid for preservation. The freeze-dried protein (100 μg) of secretion between 13-20 min were further dissolved in 95 μL of 25 mM ammonium bicarbonate ($NH_4HCO_3$). A dilute trypsin solution (Worthington trypsin, 100 ng/mL in 0.001 mol/L HCl, 5 μL) was added to 95 μL the secretion protein and mixed (trypsin: protein = 1 : 50). After overnight incubation at 37 °C, the reducing agent dithiothreitol (DTT, final concentration of 10 mM) was added and incubated at 50 °C for 30 min. The reaction system was cooled to room temperature and iodoacetamide was added to a final concentration of 40 mM, then incubated for another 30 minutes without exposure to light. The components of samples were further identified by EASY-nano LC system coupled online with Q Exactive HF mass spectrometer. The components were confirmed by Proteome Discoverer against fungus protein databases of *M. canis* from Uniprot and PDB.

**Oxidative refolding and MS identification**

The reduced peptide was synthesized by China Peptides (China), and the purity was greater than 95%. To form intermolecular disulfide bridges via oxidative refolding, the reduced peptide micansin 1 mg was dissolved in 1 mL 0.1 mol/L Tris-HCl buffer, which the pH value of the solution was adjusted to 0.5-0.8 less than the isoelectric point of the peptide, and incubated in thermostatic shaker at 28 °C for 60 h with continuous shaking at 60 rpm. The oxidized peptide solution was centrifuged at 8,000 rpm for 5 min at 4 °C, and almost immediately the supernatant was desalinated and purified by RP-HPLC (Agilent, USA) with a semipreparative C18 column (Agilent, 5 μm, 4.6 × 150 mm) using the solvent system of 0.1% TFA in water and acetonitrile containing 0.1% TFA (A) a linear gradient of 5-95% solvent A in 60 min at a constant flow rate of 1 mL/min

at 25 °C.

Matrix assisted laser desorption ionization time of flight mass (MALDI-TOF MS) (Bruker, Germany) was used to confirm the average molecular mass of the oxidative peptide. The cyclized peptide, desalinated and purified from RP-HPLC, was mixed with MALDI-matrix solution (1 mL, containing 10 mg/mL α-cyano-4-hydroxycinnamic acid (CHCA), 0.1% trifluoroacetic acid (TFA) and 50% acetonitrile). The mass of the oxidized peptide was measured using a positive-ion reflection mode.

**Determination of secondary structure**

According to the previous method, the secondary structures of peptides were determined by circular dichroism (CD) spectroscopy using a JASCO J-810 spectrometer (JASCO International Co., Ltd, Japan). All peptides were dissolved in Milli-Q water at the concentration of approximately 200 μg/mL. The CD spectra were recorded at wavelengths from 190 to 260 nm at room temperature (25 °C). The scanning speed was 50 nm/min at a 0.1 nm resolution, and the response time was set at 2 s. Each reading was repeated three times, and the results were shown as the mean residue molar ellipticity (θ). The CD spectra were quantitatively analyzed by the CDNN method using Applied Photophysics software.

**Knockout mice**

MrgprC11-knockout mice were recently created and prepared by our group (23). Mrgprb2-knockout mice were generated by the following strategy. The Mrgprb2 gene located on chromosome 7 of mice has one transcript. According to the structure of Mrgprb2 gene, exon2 of Mrgprb2-201 (ENSMUST00000052730.2) transcript is recommended as the knockout region. The region contains start codon ATG. Knockout of the region will result in disruption of protein function. The 4315 bp region including exon of Mrgprb2 was deleted on mouse chromosome 7 by GemPharmatech company using CRISPR/Cas9 technology. The brief process is as follows: sgRNA was transcribed *in vitro*. Cas9 and sgRNA were microinjected into the fertilized eggs of

C57BL/6J mice. Fertilized eggs were transplanted to obtain positive F0 mice which were confirmed by PCR and sequencing. A stable F1 generation mouse model was obtained by mating positive F0 generation mice with C57BL/6J mice. Mice genotypes were identified by PCR with two pairs of designed primers. After these mice were propagated and genetically identified for several months, enough Mrgprb2 knockout homozygous mice were gained for animal experiments.

**Acute itch behavioral tests**

Wild-type C57BL/6J mice were purchased from Disease Control and Prevention Center of Hubei Province in China. MrgprC11-knockout and Mrgprb2-knockout mice were also C57BL/6 background. All mice used in animal experiments were 6 to 12 weeks old and weighed 20 to 30 g. In the nape model, fungal peptides or secretions (50 μL) were subcutaneously injected into the nape of the mice after acclimatization. In the cheek model, saline and micasin-Ox (10 μL) were subcutaneously injected into the cheek of the mice. A scratching behavior was defined as a single hind paw stroking the site of the injection. A wipping behavior was defined as a single forepaw stroking the site of the injection. Scratching and wipping behavior in mice was observed for 30 min following injection. Some antagonists were given intraperitoneally 30 minutes prior to injection of test compound: H1R inhibitor, cetirizine (CETY), 30 mg/kg; H4R inhibitor, JNJ7777120, 40 mg/kg; Mast cell stabilizer, sodium cromoglycate, 25 mg/kg; MrgprA3 inhibitor, Berbamine (BBM), 30 mg/kg. MrgprA1 inhibitor, QWF (1 mg/kg) was used by co-injection with test compound. The vehicle used to dissolve CETY and sodium cromoglycate was saline. The vehicle (5% DMSO + 20% PEG300 + 5% Tween 80 + 70% saline) was used to dissolve JNJ7777120 and BBM. The vehicle (5% DMSO + 95% saline) was used to dissolve QWF. All experiments were approved from Animal Experiment Center, College of Life Sciences, Wuhan University and the Institutional Animal Care and Use Committee of Wuhan University (WDSKY0201707-2). All experiments were performed under the policies and recommendations of the institution and committee.

**DRG isolation and culture**

The spinal column of 4- to 5-week-old mice was removed and placed in ice-cold $Ca^{2+}$/$Mg^{2+}$-free HBSS. Dorsal root ganglion (DRG) were dissected and digested for 20 min at 37℃ in DRG digestive enzyme Mix 1 and 2 respectively. The DRG digestive enzyme Mix 1 : 1 mL $Ca^{2+}$/$Mg^{2+}$-free HBSS containing 2 μL saturated $NaHCO_3$, 0.35 mg L-cysteine, and 20 U papain. The DRG digestive enzyme Mix 2: 1 mL $Ca^{2+}$/$Mg^{2+}$-free HBSS containing 4 mg collagenase type II (Sigma) and 1.25 mg dispase type II (Roche). After digestion, neurons were pelleted, suspended in Neurobasal Plus medium (Thermo) containing 10% FBS (Gibco), 2% B-27 supplement (Thermo), 1% L-glutamine, 100 U/mL penicillin plus 100 μg/mL streptomycin, and 50 ng/mL nerve growth factor (NGF). Then neurons were plated on 8×8 mm coverslip coated with poly-D-lysine (10 μg/mL), and cultured in an incubator at 37 °C, and used within 18 h used for $Ca^{2+}$ imaging.

**qPCR**

After tissue grinding of isolated mouse DRG neurons in Trizol reagent (Takara), RNA was extracted by using chloroform and isopropanol. cDNA was gained by Reverse transcription kit (HiScript III RT SuperMix for qPCR, Vazyme). Relative mRNA expression of various Mrgprs gene were obtained by qPCR instrument (Bio-Rad CFX96) and ChamQ SYBR qPCR Master Mix Kit (Vazyme). ΔΔCt method was used to data analysis. qPCR primers were presented in Table 1.

**HEK293T cell culture and transfection**

HEK293T cells were cultured on poly-D-lysine-coated glass coverslips in DMEM high glucose medium with 10% FBS and penicillin (100 U/mL)/streptomycin (100 μg/mL). Mouse or human Mrgprs plasmids were transfected into HEK293T cells with lipofectamin 2000. Cells were replated onto glass coverslides 20 h after transfection and used for $Ca^{2+}$ imaging. Various MRGPRs plasmids carrying GFP protein tags were

used to determine $EC_{50}$ values of MRGPRs responding to Micasin-Ox. Activation ratio = Micasin-responsive cell/ GFP-expressed cell.

**Calcium imaging**

Cultured DRG neurons or HEK293T cells were loaded with 10 μM Fura-2AM (Invitrogen) or 5 μM Fluo-4AM for 30-45 min in the dark, supplemented with 0.01% Pluronic F-127 (wt/vol, Invitrogen), in 1× hank's balanced salt solution (HBSS) containing 140 mM NaCl, 5 mM KCl, 10 mM HEPES, 2 mM $CaCl_2$, 2 mM $MgCl_2$ and 10 mM d-(+)-glucose (pH 7.4). After washing 3 times with HBSS, emission at 510 nm was detected from 340 nm and 380 nm excitation for Fura-2AM. 488 nm and 520 nm were used as excitation wavelength and detection wavelength for Fluo-4AM. Data were analyzed from at least three repeated experiments and 80-200 cells.

**Evans blue analysis**

Adult male C57BL/6 mice were anesthetized by intraperitoneal injection of 0.1 mL chloral hydrate (7%). Fifteen minutes after induction of anesthesia, the mice were injected with 50 μL 12.5 mg/mL evans blue (Sigma) in saline through the tail vein. Ten minutes after Evans blue injection, the test substance (5 μL) was intraplantarly injected into one hindpaw of each mouse, and saline (5 μL) was injected into the other hindpaw. Mice were sacrificed 15 minutes after paw injections by $CO_2$ inhalation and decapitation. The hindpaws of the mice were imaged, and paw tissues were collected, dried for 24 h at 50 °C, and weighed. Evans blue was extracted by 24-hour incubation in formamide at 50 °C, and the OD values were read at 620 nm using a spectrophotometer. The concentration of Evans blue dye was determined based on the corresponding standard curve and expressed as ng/mg of tissue weight.

## Data Availability Statement

No datasets were generated or analyzed during the current study.

## Conflict of Interest

The authors declare that they have no relevant conflicts of interest.

## Acknowledgments

We thank Dr. Qin Liu and Dr. Weishan Yang (Washington University School of Medicine, St Louis, Mo) for their valuable communications with us. We also thank Dr. Yan Zhou (Medical Research Institute of Wuhan University, China) for providing human brain cDNAs to clone MrgprXs genes. This study was funded by National Science Fund of China [Nos. 32070525 and 32161160303], National Key Research and Development Program of China [No. 2023YFF1304900], Shenzhen Science and Technology Program of China [Nos. JCYJ20220530140800001 and JCYJ20230807090212024], and Hubei University of Technology High-level Talent Launch Fund [No. GCC2024009].



## Author contributions

Conceptualization: H. Y. and Z. C.; Data curation: H. Y., Y. C., Y. W. and Z. C.; Formal Analysis: L. W. and H. K.; Funding acquisition: Z. C.; Investigation: H. Y.; Methodology: H. Y., H. K. and Z. C.; Project administration: H. Y. and Y. C.; Visualization: H. Y. and Y. C.; Writing – original draft: H. Y.; Writing – review & editing: H. Y., Y.W. and Z. C.; Resources: Y.W. and Z. C.; Software: L. W., B. G., L. Y. and R. R.; Supervision: H. K. and Z. C.; Validation: Y.W. and Z. C.

Table 1 qPCR primers of Mrgprs

| Primer name | Sequence (5'-3') |
|---|---|
| MrgprA1-qPCR-F | CTCGCCAACAGCACCCACAAC |
| MrgprA1-qPCR-R | GCCCAGGAGCCAGAACACAATG |
| MrgprA2-qPCR-F | CAGCCTCACCAACAGCACCAG |
| MrgprA2-qPCR-R | TCAGTCCGACCAGTCCGAAGATG |
| MrgprA3-qPCR-F | ACACAAGCCAGCAAGCTACA |
| MrgprA3-qPCR-R | ACTTCCAGGGATGGTTTCGT |
| MrgprB4-qPCR-F | TCACTGCCAAAGACCAAGACACAC |
| MrgprB4-qPCR-R | AACCACAGCCTAGCCCTACCAC |
| MrgprB5-qPCR-F | CTTCTTCAGAGAGCCATGCAGGAC |
| MrgprB5-qPCR-R | TTTCCAGTTCCCCAGACCTTTGTG |
| MrgprC11-qPCR-F | AGCATCCACAACCCCAGAAG |
| MrgprC11-qPCR-R | TGGAGTGCAGTTGGGATGAC |
| mouse-Actin-qPCR-F | CGTCGACAACGGCTCCGGCATG |
| mouse-Actin-qPCR-R | CCACCATCACACCCTGGTGCCTAGG |



## References

Al Hamwi G, Riedel YK, Clemens S, Namasivayam V, Thimm D, Müller CE. MAS-related G protein-coupled receptors X (MRGPRX): Orphan GPCRs with potential as targets for future drugs. Pharmacol Ther 2022;238:108259.

Andoh T, Takayama Y, Yamakoshi T, Lee J-B, Sano A, Shimizu T, et al. Involvement of Serine Protease and Proteinase-Activated Receptor 2 in Dermatophyte-Associated Itch in Mice. Journal of Pharmacology and Experimental Therapeutics 2012;343(1):91-6.

Azimi E, Reddy VB, Shade KTC, Anthony RM, Talbot S, Pereira PJS, et al. Dual action of neurokinin-1 antagonists on Mas-related GPCRs. Jci Insight 2016;1(16):e89362.

Bader M, Alenina N, Andrade-Navarro MA, Santos RA. MAS and its related G protein-coupled receptors, Mrgprs. Pharmacol Rev 2014;66(4):1080-105.

Bi K, Liang Y, Mengiste T, Sharon A. Killing softly: a roadmap of Botrytis cinerea pathogenicity. Trends Plant Sci 2023;28(2):211-22.

Cevikbas F, Lerner EA. Physiology and Pathophysiology of Itch. Physiol Rev 2020;100(3):945-82.

Chanyachailert P, Leeyaphan C, Bunyaratavej S. Cutaneous Fungal Infections Caused by Dermatophytes and Non-Dermatophytes: An Updated Comprehensive Review of Epidemiology, Clinical Presentations, and Diagnostic Testing. J Fungi (Basel) 2023;9(6).

Chen XQ, Yu J. Global Demographic Characteristics and Pathogen Spectrum of Tinea Capitis.

Mycopathologia 2023.

Chen XQ, Zheng DY, Xiao YY, Dong BL, Cao CW, Ma L, et al. Aetiology of tinea capitis in China: a multicentre prospective study*. British Journal of Dermatology 2021;186(4):705-12.

Chermette R, Ferreiro L, Guillot J. Dermatophytoses in animals. Mycopathologia 2008;166(5-6):385-405.

Cole DC, Govender NP, Chakrabarti A, Sacarlal J, Denning DW. Improvement of fungal disease identification and management: combined health systems and public health approaches. Lancet Infect Dis 2017;17(12):e412-e9.

Cosi V, Gadermaier G. The Role of Defensins as Pollen and Food Allergens. Curr Allergy Asthma Rep 2023;23(6):277-85.

Descamps F, Brouta F, Monod M, Zaugg C, Baar D, Losson B, et al. Isolation of a Microsporum canis gene family encoding three subtilisin-like proteases expressed in vivo. J Invest Dermatol 2002;119(4):830-5.

Dhaille F, Dillies AS, Dessirier F, Reygagne P, Diouf M, Baltazard T, et al. A single typical trichoscopic feature is predictive of tinea capitis: a prospective multicentre study. British Journal of Dermatology 2019;181(5):1046-51.

Dong X, Dong X. Peripheral and Central Mechanisms of Itch. Neuron 2018;98(3):482-94.

Gan B, Yu L, Yang H, Jiao H, Pang B, Chen Y, et al. Mechanism of agonist-induced activation of the human itch receptor MRGPRX1. PLoS Biol 2023;21(6):e3001975.

Gnat S, Łagowski D, Nowakiewicz A, Dyląg M. A global view on fungal infections in humans and animals: infections caused by dimorphic fungi and dermatophytoses. Journal of Applied Microbiology 2021;131(6):2688-704.

Guo L, Zhang Y, Fang G, Tie L, Zhuang Y, Xue C, et al. Ligand recognition and G protein coupling of the human itch receptor MRGPRX1. Nat Commun 2023;14(1):5004.

Gupta K, Kotian A, Subramanian H, Daniell H, Ali H. Activation of human mast cells by retrocyclin and protegrin highlight their immunomodulatory and antimicrobial properties. Oncotarget 2015;6(30):28573-87.

Guryanova SV, Ovchinnikova TV. Immunomodulatory and Allergenic Properties of Antimicrobial Peptides. Int J Mol Sci 2022;23(5).

Hu J, Wang L, Yang H, Meng Y, Tao M, Wu Y, et al. Key domains and residues of the receptor MRGPRX1 recognizing the peptide ligand BAM8-22. Peptides 2023;161:170927.

Kromer C, Celis D, Hipler UC, Zampeli VA, Mößner R, Lippert U. Dermatophyte infections in children compared to adults in Germany: a retrospective multicenter study in Germany. JDDG: Journal der Deutschen Dermatologischen Gesellschaft 2021;19(7):993-1001.

Lay M, Dong X. Neural Mechanisms of Itch. Annual Review of Neuroscience 2020;43(1):187-205.

Li X, Yang H, Han Y, Yin S, Shen B, Wu Y, et al. Tick peptides evoke itch by activating MrgprC11/MRGPRX1 to sensitize TRPV1 in pruriceptors. J Allergy Clin Immunol 2021;147(6):2236-48.e16.

Lima AM, Azevedo MIG, Sousa LM, Oliveira NS, Andrade CR, Freitas CDT, et al. Plant antimicrobial peptides: An overview about classification, toxicity and clinical applications. Int J Biol Macromol 2022;214:10-21.

Liu Q, Tang Z, Surdenikova L, Kim S, Patel KN, Kim A, et al. Sensory neuron-specific GPCR Mrgprs are itch receptors mediating chloroquine-induced pruritus. Cell 2009;139(7):1353-65.

Liu Y, Cao C, Huang XP, Gumpper RH, Rachman MM, Shih SL, et al. Ligand recognition and allosteric

modulation of the human MRGPRX1 receptor. Nat Chem Biol 2023;19(4):416-22.

Lund A, DeBoer DJ. Immunoprophylaxis of Dermatophytosis in Animals. Mycopathologia 2008;166(5-6):407-24.

Martinez-Rossi NM, Peres NTA, Bitencourt TA, Martins MP, Rossi A. State-of-the-Art Dermatophyte Infections: Epidemiology Aspects, Pathophysiology, and Resistance Mechanisms. J Fungi (Basel) 2021;7(8).

McNeil BD, Pundir P, Meeker S, Han L, Undem BJ, Kulka M, et al. Identification of a mast-cell-specific receptor crucial for pseudo-allergic drug reactions. Nature 2015;519(7542):237-41.

Meixiong J, Anderson M, Limjunyawong N, Sabbagh MF, Hu E, Mack MR, et al. Activation of Mast-Cell-Expressed Mas-Related G-Protein-Coupled Receptors Drives Non-histaminergic Itch. Immunity 2019a;50(5):1163-71.e5.

Meixiong J, Vasavda C, Green D, Zheng Q, Qi L, Kwatra SG, et al. Identification of a bilirubin receptor that may mediate a component of cholestatic itch. Elife 2019b;8.

Meixiong J, Vasavda C, Snyder SH, Dong X. MRGPRX4 is a G protein-coupled receptor activated by bile acids that may contribute to cholestatic pruritus. Proc Natl Acad Sci U S A 2019c;116(21):10525-30.

Moriello KA, Coyner K, Paterson S, Mignon B. Diagnosis and treatment of dermatophytosis in dogs and cats. Veterinary Dermatology 2017;28(3):266-e68.

Moskaluk AE, VandeWoude S. Current Topics in Dermatophyte Classification and Clinical Diagnosis. Pathogens 2022;11(9).

Nakamura T, Yoshida N, Anzawa K, Nishibu A, Mochizuki T. Itching in a trichophytin contact dermatitis mouse model and the antipruritic effect of antifungal agents. Clinical and Experimental Dermatology 2018;44(4):381-9.

Ng TB, Cheung RC, Wong JH, Ye XJ. Antimicrobial activity of defensins and defensin-like peptides with special emphasis on those from fungi and invertebrate animals. Curr Protein Pept Sci 2013;14(6):515-31.

Paryuni AD, Indarjulianto S, Widyarini S. Dermatophytosis in companion animals: A review. Vet World 2020;13(6):1174-81.

Reddy VB, Sun S, Azimi E, Elmariah SB, Dong X, Lerner EA. Redefining the concept of protease-activated receptors: cathepsin S evokes itch via activation of Mrgprs. Nat Commun 2015;6:7864.

Ryu K, Heo Y, Lee Y, Jeon H, Namkung W. Berbamine Reduces Chloroquine-Induced Itch in Mice through Inhibition of MrgprX1. International Journal of Molecular Sciences 2022;23(22).

Segal E, Elad D. Human and Zoonotic Dermatophytoses: Epidemiological Aspects. Front Microbiol 2021;12:713532.

Selsted ME, Ouellette AJ. Mammalian defensins in the antimicrobial immune response. Nat Immunol 2005;6(6):551-7.

Simons FER, Simons KJ. Histamine and H1-antihistamines: Celebrating a century of progress. Journal of Allergy and Clinical Immunology 2011;128(6):1139-50.e4.

Subramanian H, Gupta K, Lee D, Bayir AK, Ahn H, Ali H. β-Defensins activate human mast cells via Mas-related gene X2. J Immunol 2013;191(1):345-52.

Suzuki R, Numata T, Hiruma J, Maeda T, Tsuboi R, Harada K. Wolf's isotopic response after tinea corporis caused by

Microsporum canis. The Journal of Dermatology 2023.

Tseng PY, Hoon MA. Specific β-Defensins Stimulate Pruritus through Activation of Sensory Neurons.

Journal of Investigative Dermatology 2022;142(3 Pt A):594-602.

Wang X, Jiang N, Liu J, Liu W, Wang GL. The role of effectors and host immunity in plant-necrotrophic fungal interactions. Virulence 2014;5(7):722-32.

Wilson SR, Gerhold KA, Bifolck-Fisher A, Liu Q, Patel KN, Dong X, et al. TRPA1 is required for histamine-independent, Mas-related G protein-coupled receptor-mediated itch. Nat Neurosci 2011;14(5):595-602.

Wolf K, Kühn H, Boehm F, Gebhardt L, Glaudo M, Agelopoulos K, et al. A group of cationic amphiphilic drugs activates MRGPRX2 and induces scratching behavior in mice. J Allergy Clin Immunol 2021;148(2):506-22.e8.

Woodfolk JA, Sung S-SJ, Benjamin DC, Lee JK, Platts-Mills TAE. Distinct Human T Cell Repertoires Mediate Immediate and Delayed-Type Hypersensitivity to the Trichophyton Antigen, Tri r 2. The Journal of Immunology 2000;165(8):4379-87.

Yang Z, Chen W, Wan Z, Song Y, Li R. Tinea Capitis by Microsporum canis in an Elderly Female with Extensive Dermatophyte Infection. Mycopathologia 2021;186(2):299-305.

Zeya HI, Spitznagel JK. Antimicrobial specificity of leukocyte lysosomal cationic proteins. Science 1966;154(3752):1049-51.

Zhan P, Liu W. The Changing Face of Dermatophytic Infections Worldwide. Mycopathologia 2016;182(1-2):77-86.

Zhang L, McNeil BD. Beta-defensins are proinflammatory pruritogens that activate Mrgprs. J Allergy Clin Immunol 2019;143(5):1960-2.e5.

Zhi H, Shen H, Zhong Y, Sang B, Lv W, Li Q, et al. Tinea capitis in children: A single-institution retrospective review from 2011 to 2019. Mycoses 2021;64(5):550-4.

Zhu S, Gao B, Harvey PJ, Craik DJ. Dermatophytic defensin with antiinfective potential. Proc Natl Acad Sci U S A 2012;109(22):8495-500.

Zhu S, Gao B, Umetsu Y, Peigneur S, Li P, Ohki S, et al. Adaptively evolved human oral actinomyces-sourced defensins show therapeutic potential. EMBO Mol Med 2022;14(2):e14499.

## Figure and figure legends

### Figure 1

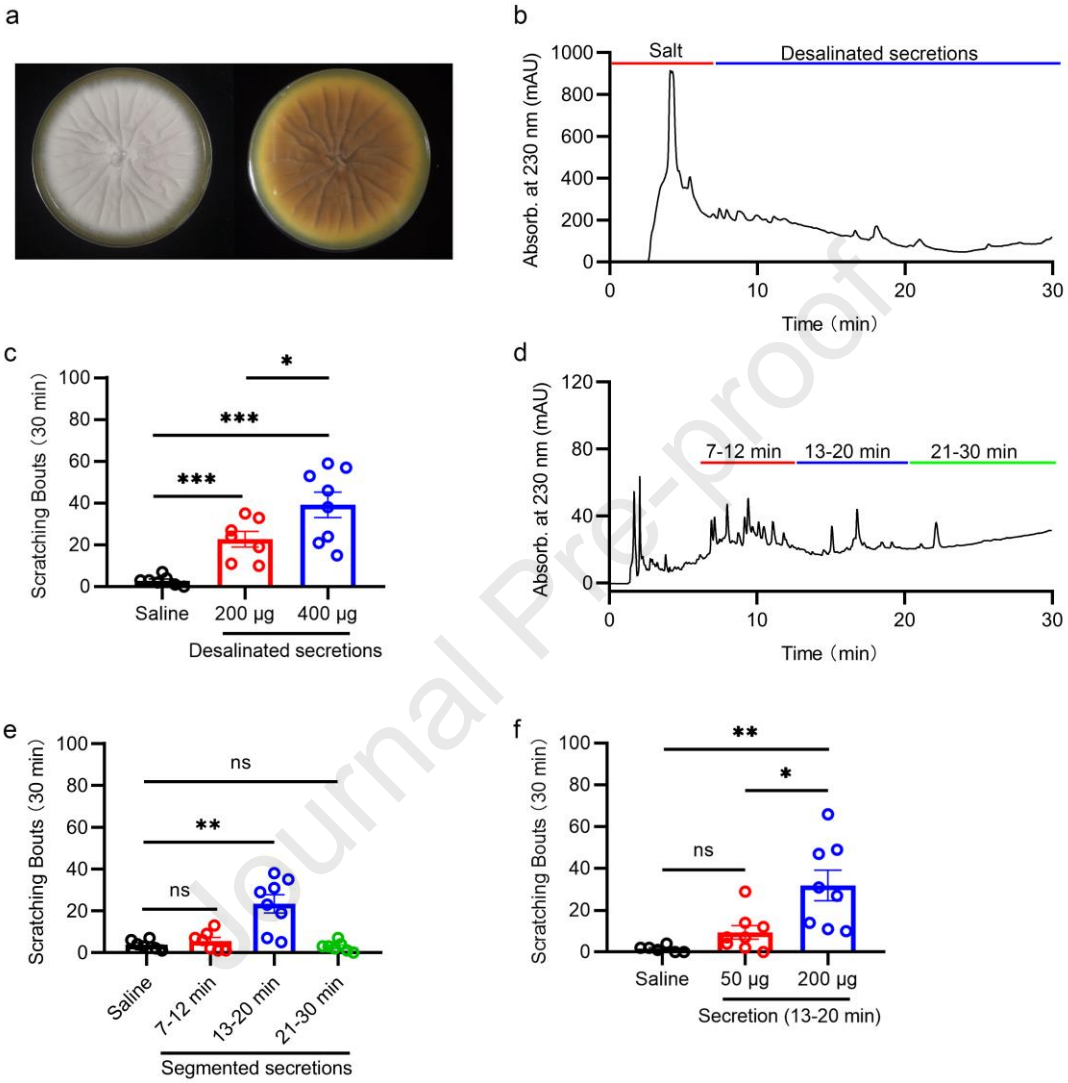


**Scratching and itching responses of mice evoked by the fungal secretion of the dermatophyte *M. canis*.**

(a), Colony morphology of the dermatophyte *M. canis* strain ATCC 10214. (b), The retention time of the supernatant containing *M. canis* secretion by RP-HPLC. The peak of 0-7 min was considered as salt component (red). The peak of 8-30 min (blue) was collected as the desalted fungal secretion. (c), Itchy effect induced by the fungal secretion of *M. canis* in wild type mice. Scratching and itching responses were caused by intradermal injection of vehicle (Saline, n = 7, black), the fungal secretion of 200 μg

(n = 7, red) and 400 μg (n = 8, blue) in wild type mice. Saline (2.85±0.85) vs 200 μg (22.71±3.75), P=0.0002; Saline (2.85±0.85) vs 400 μg (39.13±6.12), P=0.0001; 200 μg (22.71±3.75) vs 400 μg (39.13±6.12), P=0.0459. (d), The retention time of the desalted *M. canis* secretion by RP-HPLC. Peaks of three time periods (7-12 min, red; 13-20 min, blue; 21-30 min, green) were collected separately. (e), Scratching bouts induced by freeze-dried samples from different retention times in the segmented fungal secretion. Every fungal secretion of 500 μg was transformed into freeze-dried samples of three time periods by RP-HPLC, each of which was dissolved in saline of 50 μL and intradermally injected into the neck of a mouse. Vehicle (Saline, n = 6, black), the freeze-dried samples of 7-12 min (n = 7, red), 13-20 min (n = 8, blue) and 21-30 min (n = 7, green). Saline (3.83±0.94) vs 7-12 min (5.57±1.72), P=0.4164; Saline (3.83±0.94) vs 13-20 min (23.38±4.36), P=0.0026; Saline (3.83±0.94) vs 21-30 min (2.86±0.86), P=0.4597. (f), Itch effect evoked by the fungal secretion (13-20 min) at different doses. Scratching bouts were caused by intradermal injection of vehicle (Saline, n = 6, black) and the fungal secretion (13-20 min) (50 μg, n = 8; 200 μg, n = 7). Saline (1.5±0.62) vs 50 μg (9.38±3.26), P=0.0629; Saline (1.5±0.62) vs 200 μg (31.88±7.25), P=0.0038; 50 μg (9.38±3.26) vs 200 μg (31.88±7.25), P=0.0134. Each dot represents an individual mouse. All data are presented as the mean ± SEM. ns, not significant, P > 0.5; *, P < 0.05; **, P < 0.01; ***, P < 0.001. Two-tailed T-test is used to calculate the p-values.

**Figure 2**

a

| Order | Accession | Description | Exp. q-value | Sum PEP Score | Coverage | # Peptides |
|---|---|---|---|---|---|---|
| 1 | XP_002844682.1 | extensin [*Microsporum canis* CBS 113480] | 0 | 57.18391673 | 34.47154472 | 11 |
| 2 | XP_002845450.1 | hsp70-like protein [*Microsporum canis* CBS 113480] | 0 | 43.63418916 | 11.62079511 | 8 |
| 3 | EEQ29258.1 | Cu, Zn superoxide dismutase [*Microsporum canis* CBS 113480] | 0 | 33.37843672 | 85.06493506 | 5 |
| 4 | 2LR5 | A Chain A, micasin | 0 | 27.94356862 | 100 | 3 |
| 5 | EEQ32886.1 | conserved hypothetical protein [*Microsporum canis* CBS 113480] | 0 | 25.9686595 | 52.05479452 | 8 |
| 6 | EEQ27779.1 | tenascin C [*Microsporum canis* CBS 113480] | 0 | 25.0766745 | 36.72654691 | 10 |
| 7 | XP_002849737.1 | antioxidant protein LsfA [*Microsporum canis* CBS 113480] | 0 | 24.58261093 | 16.28959276 | 6 |
| 8 | EEQ33402.1 | conserved hypothetical protein [*Microsporum canis* CBS 113480] | 0 | 21.29127406 | 16.30434783 | 3 |
| 9 | XP_002843445.1 | conserved hypothetical protein [*Microsporum canis* CBS 113480] | 0 | 16.27992768 | 22.68041237 | 4 |
| 10 | XP_002846678.1 | stress protein DDR48 [*Microsporum canis* CBS 113480] | 0 | 12.08446407 | 31.96480938 | 6 |

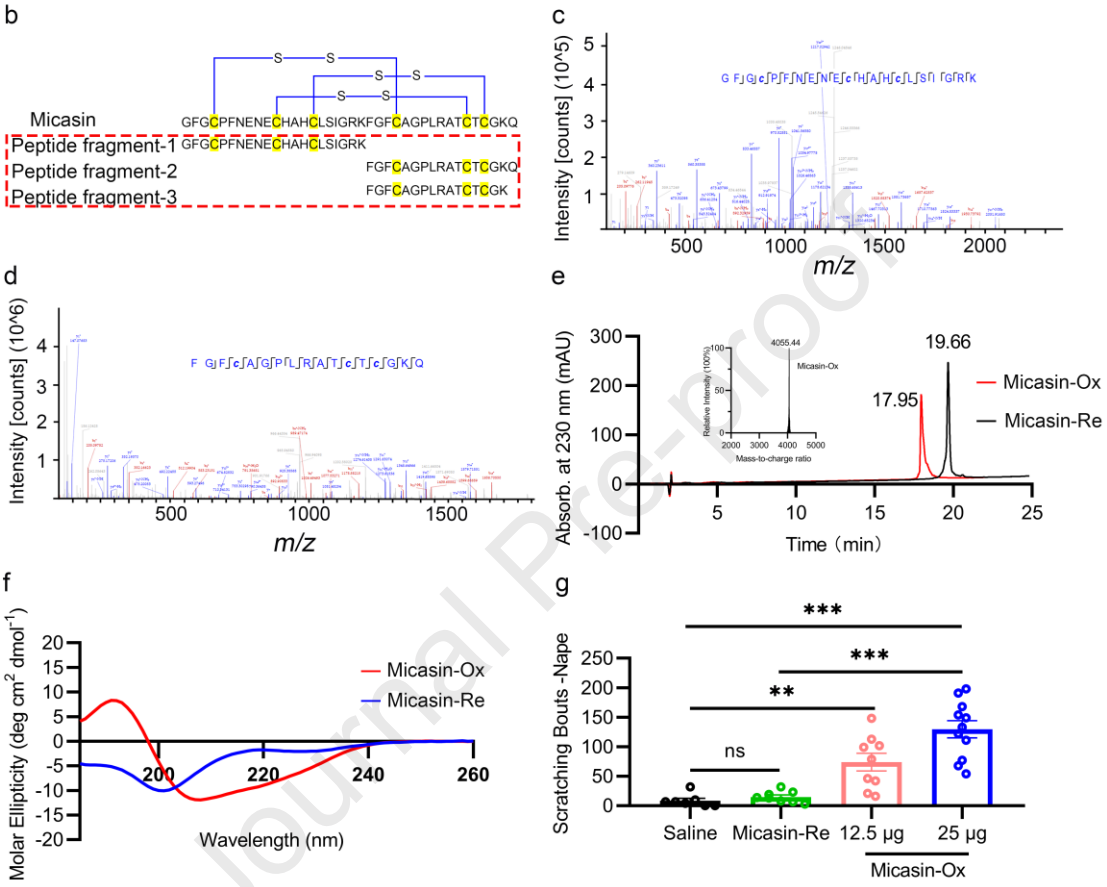


**Itch effect of the peptide micasin secreted from *M. canis* on mice by directly activating itch-sensing neurons.**

(a), The top 10 components of Sum PEP Score in fungal secretion identified by LC–MS/MS method. These components were ranked based on Sum PEP Score. Sum PEP Score was the comprehensive score based on the identified protein quality and abundance. Exp. q-value represented the matching credibility of the identified protein to the proteins in the protein library. The lower q-value had the higher the credibility of the match. Coverage showed the percentage of identified protein fragments in the total length of the protein in the protein library. # Peptides was the number of identified protein fragments. (b-d), Identified peptide fragments covering the full-length amino

acid sequences of micasin by LC–MS/MS method. Three peptide fragments were identified from the secretion of *M. canis* by LC–MS/MS combined with Proteome Discoverer searching (b). The representative N-terminal (c) and C-terminal (d) of the peptide micasin were identified. Relative abundance and intensity of peptides are shown as percentages on Y-axis. The amino acid sequences are confirmed by analyzing molecular weight of bn and yn ions. (e), The retention time analysis of the peptide micasin before and after oxidative refolding by RP-HPLC and MALDI-TOF MS analysis of the oxidized micasin (Micasin-Ox). The absorption of Micasin-Ox and the reduced micasin (Micasin-Re) at 230 nm are presented as red and black curves, respectively. (f), Comparison of secondary structure of Micasin-Re (blue) vs Micasin-Ox (red) by circular dichroism spectrum analysis. (g), Dose-dependent scratching responses elicited by intradermal injection of Micasin-Ox, Saline (n = 7), Micasin-Re (25 μg, n = 8) and Micasin-Ox (12.5 μg, n = 9; 25 μg, n = 11). Saline (8.57±4.15) vs Micasin-Re (14.88±3.35), P=0.25; Saline (8.57±4.15) vs 12.5 μg Micasin-Ox (74±15.10), P=0.0023; Saline (8.57±4.15) vs 25 μg Micasin-Ox (129.50±14.64), P<0.0001; 25 μg Micasin-Re (14.88±3.35) vs 25 μg Micasin-Ox (129.50±14.64), P<0.0001. Each dot represents an individual mouse. All data are presented as the mean ± SEM. ns, not significant, P > 0.5; **, P < 0.01; ***, P < 0.001. Two-tailed T-test is used to calculate the p-values.

**Figure 3**

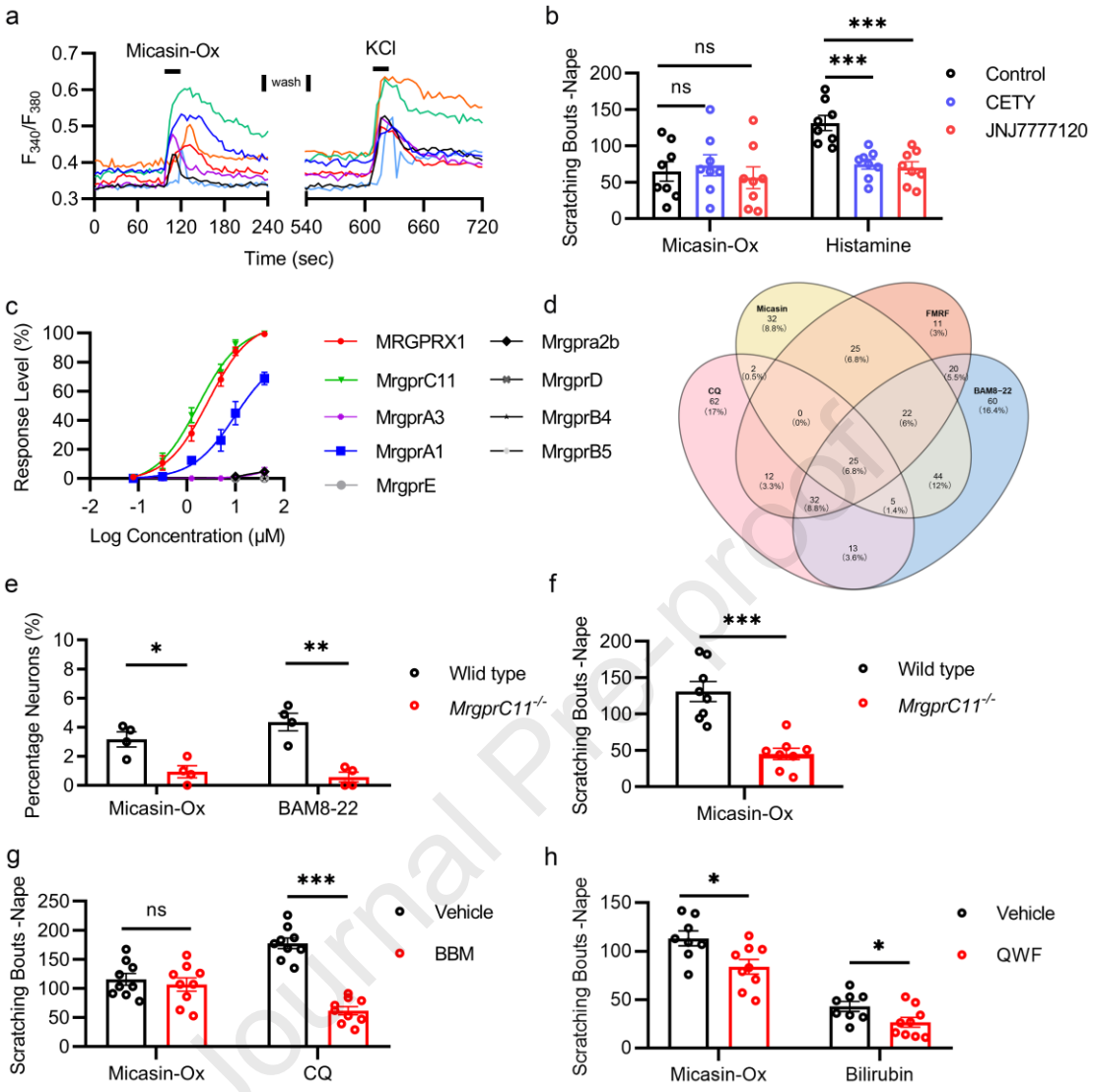


**Non-histaminergic itch elicited by Micasin-Ox activating MRGPRX1/C11 on pruriceptors.**

(a), Representative calcium traces of the cultured mouse DRG neurons in the presence of Micasin-Ox (10 μM). KCl (50 mM) was used as the positive control. (b), Scratching responses induced by intradermal injection of Micasin-Ox (25 μg) after 30 minutes of intraperitoneal injection with control (saline, black), H1R inhibitor cetirizine (CETY, blue) and H4R inhibitor JNJ7777120 (red) in WT mice. Histamine (HIS, 10 μmol) was used as a positive control. Each dot represents an individual mouse, n ≥ 6. Micasin-Ox: Control (64.88±13.42) vs CETY (73.38±14.55), P=0.674; Control (64.88±13.42) vs JNJ7777120 (56.25±15.11), P=0.676. Histamine: Control (131.4±10.35) vs CETY

(74.75±6.83), P=0.0004; Control (131.4±10.35) vs JNJ7777120 (70.13±8.21), P=0.0004. (c), $EC_{50}$ values of MRGPRs responding to Micasin-Ox. Various MRGPRs plasmids carrying GFP protein tags were used to determine $EC_{50}$ values of MRGPRs responding to Micasin-Ox. Cells with an increase of F340/F380 baseline of more than 50% were counted as micasin-responsive cells. Response level was the ratio of micasin-responsive cells to GFP-positive cells. At least 80-200 cells under a 20× field were used for data analysis in each repeated experiment. MRGPRX1, MrgprC11, MrgprA3 and MrgprA1 (Concentration of Micasin-Ox, 0.0781, 0.312, 1.25, 5, 10 and 40 μM); Mrgpra2b, MrgprB4, MrgprB5, MrgprD, MrgprE (10 and 40 μM). MRGPRX1, $EC_{50}$=2.75 μM, response level at Micasin-Ox (40 μM), 99.46±0.22%, n=3; MrgprC11, $EC_{50}$=1.71 μM, response level at Micasin-Ox (40 μM), 99.54±0.11%, n=3; MrgprA1, $EC_{50}$=9.69 μM, response level at Micasin-Ox (40 μM), 68.83±2.47%, n=3; MrgprA3, $EC_{50}$=n.d., response level at Micasin-Ox (40 μM), 5.00±1.42%, n=3; Mrgpra2b, response level at Micasin-Ox (40 μM), 4.73±1.02%, n=3; MrgprB4, response level at Micasin-Ox (40 μM), 0±0%, n=3; MrgprB5, response level at Micasin-Ox (40 μM), 0±0%, n=3; MrgprD, response level at Micasin-Ox (40 μM), 0±0%, n=3; MrgprE, response level at Micasin-Ox (40 μM), 0±0%, n=3. n.d. indicates an $EC_{50}$ value that could not be estimated from the fitted data. All data are presented as the mean ± SEM. (d), Venn diagram analysis of co-activation ratio of micasin and other Mrgpr ligands on mouse DRG neurons. (e), Quantification of calcium imaging assay on the cultured DRG neurons from WT and MrgprC11-knockout (*MrgprC11*$^{-/-}$) mice in the presence of Micasin-Ox. The vertical axis represents the ratio of the number of DRG neurons activated by different ligands (Micasin-Ox, 10 μM; BAM8-22, 10 μM) to the number of DRG neurons activated by KCl (50 mM). Micasin-Ox: Wild type (3.16±0.52) vs *MrgprC11*$^{-/-}$ (0.94±0.41), P=0.015; BAM8-22: Wild type (4.36±0.59) vs *MrgprC11*$^{-/-}$ (0.57±0.33), P=0.0015. At each dot, at least 200 DRG neurons were counted under a 10× field, n=4. (f), Scratching responses induced by intradermal injection of Micasin-Ox (25 μg) in WT (n = 8) and MrgprC11-knockout (*MrgprC11*$^{-/-}$) (n = 8) mice. Wild type (130.9±13.77) vs *MrgprC11*$^{-/-}$ (45±7.74), P=0.0001. (g), Difference of scratching

responses induced by intradermal injection of Micasin-Ox (25 μg) and CQ (200 μg) after 30 minutes of intraperitoneal injection with vehicle (5% DMSO + 20% PEG300 + 5% Tween 80 + 70% saline, black) and MrgprA3 inhibitor Berbamine (BBM) (red, 30 mg/kg) in WT mice. Micasin-Ox: Vehicle (115.4±10.02) vs BBM (106.8±11.43), P=0.576. CQ: Vehicle (177.6±9.23) vs BBM (61.67±7.08), P<0.0001. Each dot represents an individual mouse, n ≥ 8. (h), Difference of scratching responses induced by intradermal co-injection of different ligands (Micasin-Ox, 25 μg; Bilirubin, 60 μg) with vehicle (5% DMSO + 95% saline, black) and MrgprA1 inhibitor QWF (red, 1 mg/kg) in WT mice. Micasin-Ox: Vehicle (113.4±7.69) vs QWF (84±7.45), P=0.015. Bilirubin: Vehicle (42.88±5.09) vs QWF (26.67±5.13), P=0.041. Each dot represents an individual mouse, n ≥ 8. All data are presented as the mean ± SEM. ns, not significant, P > 0.5; *, P < 0.05; **, P < 0.01; ***, P < 0.001. Two-tailed T-test is used to calculate the p-values.

**Figure 4**

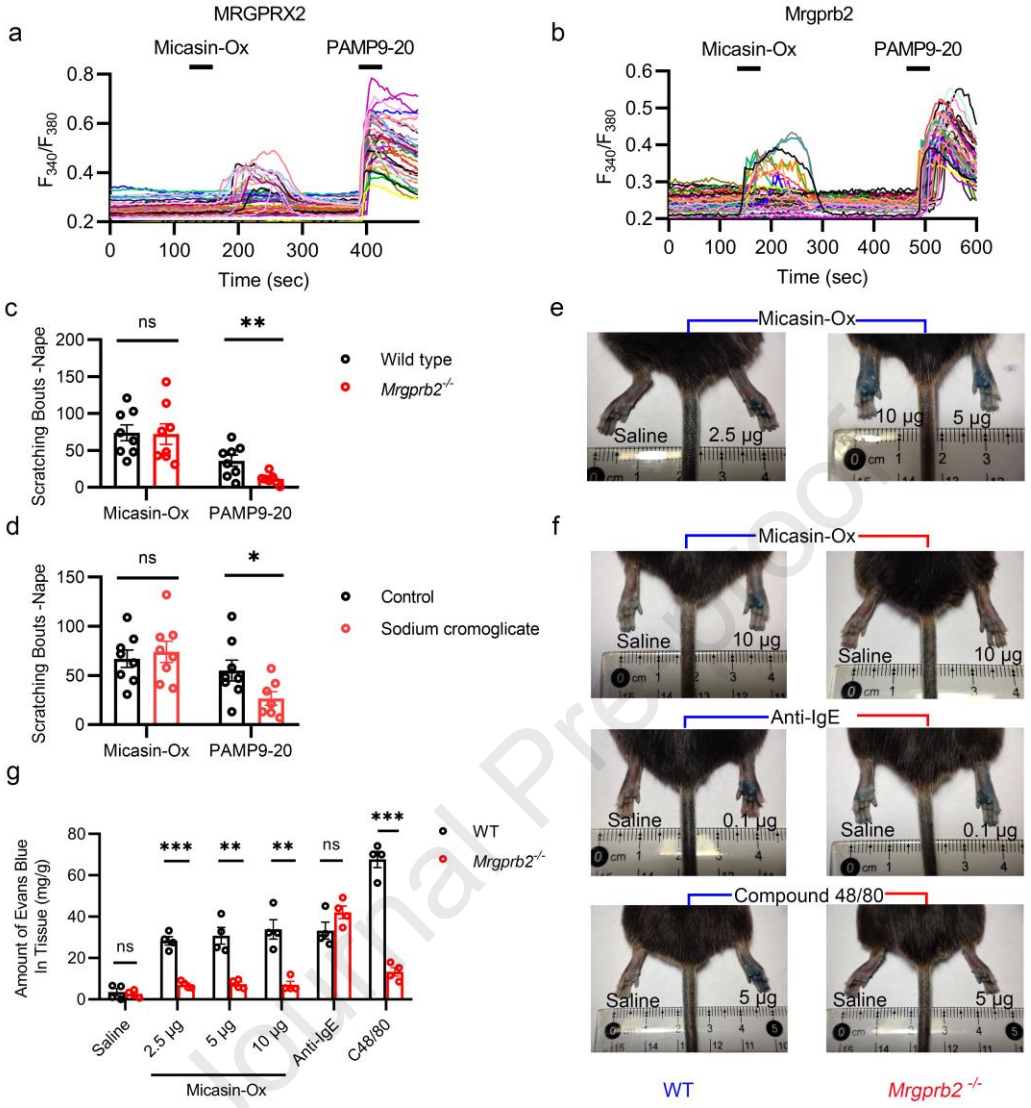


**Inflammation rather than itch triggered by Micasin-Ox activating MRGPRX2/b2.** (a-b), Representative calcium traces of MRGPRX2 (a) and Mrgprb2 (b) -overexpressed HEK293T cells responding to Micasin-Ox (10 μM). PAMP9-20 (10 μM) was used as the positive control. (c), Difference of scratching responses induced by intradermal injection of Micasin-Ox (25 μg) and the Mrgprb2 agonist PAMP9-20 (50 μg) in WT (Micasin-Ox, n = 8; PAMP9-20, n = 8) and Mrgprb2-knockout (*Mrgprb2*$^{-/-}$) (Micasin-Ox, n = 8; PAMP9-20, n = 8) mice. Each dot represents an individual mouse. Micasin-Ox: Wild type (73.87±10.83) vs Mrgprb2-knockout (72.25±13.95), P=0.928; PAMP9-20: Wild type (36±7.56) vs Mrgprb2-knockout (11.5±2.42), P=0.008.(d), Difference of scratching responses induced by intradermal injection of Micasin-Ox (25 μg) and

PAMP9-20 (50 μg) after 30 minutes of intraperitoneal injection with control (saline, black) and mast cell degranulation inhibitor, sodium cromoglycate (red) in WT mice. Each dot represents an individual mouse (n ≥ 6). Micasin-Ox: Control (67±8.82) vs Sodium cromoglicate (74.12±10.87), P=0.618; PAMP9-20: Control (55±10.62) vs Sodium cromoglicate (26.57±6.95), P=0.0493. (e), Representative images of evans blue stained extravasation 15 min after intraplantar injection of Micasin-Ox (2.5 μg, 5 μg and 10 μg) in wild type mice. Saline was used as the negative control. (f), Difference of evans blue extravasation in paws of wild type (blue) and Mrgprb2 knockout (red) mice after subcutaneous injection of Micasin-Ox. The left paw subcutaneously injected into saline was used as the negative control. The right paw subcutaneously injected into Anti-IgE, compound 48/80 and Micasin-Ox. Anti-IgE (1 μg) and compound 48/80 (0.1 μg) were the positive controls. (g), Evans blue quantitative assay of paws after injection of Anti-IgE, compound 48/80 and Micasin-Ox in wild type (black) and Mrgprb2 (red) knockout mice. Saline: Wild type (3.52±1.73) vs Mrgprb2 KO (2.70±0.86), P=0.6885; Micasin-Ox (2.5 μg): Wild type (28.23±2.03) vs Mrgprb2 KO (7.08±0.85), P <0.0001; Micasin-Ox (5 μg): Wild type (30.80±4.07) vs Mrgprb2 KO (7.41±1.05), P=0.0014; Micasin-Ox (10 μg): Wild type (33.68±4.68) vs Mrgprb2 KO (7.05±1.68), P=0.0017; Anti-IgE: Wild type (33.29±4.07) vs Mrgprb2 KO (42.11±3.06), P=0.1345; C48/80: Wild type (67.67±3.90) vs Mrgprb2 KO (13.32±2.06), P<0.0001. Wild type: Saline (3.52±1.73) vs Micasin-Ox (2.5 μg) (28.23±2.03), P<0.0001; Saline (3.52±1.73) vs Anti-IgE (33.29±4.07), P=0.0005; Saline (3.52±1.73) vs C48/80 (67.67±3.90), P<0.0001. All data are presented as the mean ± SEM. ns, not significant, P > 0.5; *, P < 0.05; **, P < 0.01; ***, P < 0.001. Two-tailed T-test is used to calculate the p-values.

**Figure 5**

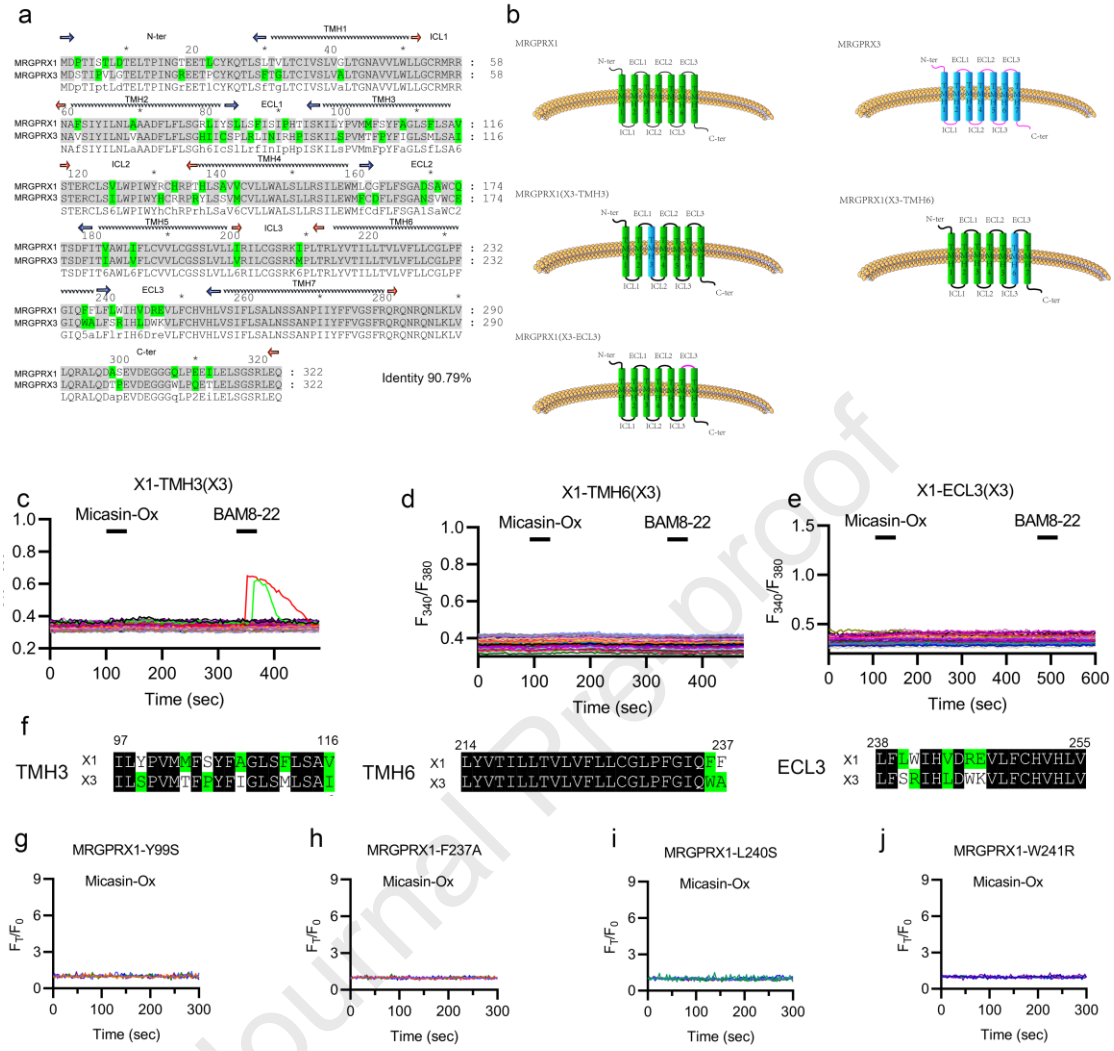


**The identification of key domains and residues in MRGPRX1 recognizing Micasin-Ox.**

(a), Alignment of amino acid sequences between hMRGPRX1 and hMRGPRX3. Green background font represented differential amino acids. (b), The topological diagrams with seven transmembrane helices of MRGPRX1, MRGPRX3 and MRGPRX1(X3-domain) chimeras. The TMHs of MRGPRX1 were green and other domains were black. The TMHs of MRGPRX3 were blue and other domains were pink. Only partial topological diagrams of MRGPRX1(X3-domain) chimeras were showed: MRGPRX1(X3-TMH3), MRGPRX1(X3-TMH6) and MRGPRX1(X3-ECL3). (c-e), Representative calcium traces of MRGPRX1(X3-TMH3) (c), MRGPRX1(X3-TMH6)

(d) and MRGPRX1(X3-ECL3) (e) -overexpressed HEK293T cells responding to Micasin-Ox (10 μM). BAM8-22 (10 μM) was used as the positive control. (f), Alignment of amino acid sequences in three domains (TMH3, TMH6 and ECL3) between MRGPRX1 and MRGPRX3. Green background font represented differential amino acids. (g-j), Representative calcium traces of point mutations in MRGPRX1-overexpressed HEK293T cells responding to Micasin-Ox (10 μM). MRGPRX1 mutants were MRGPRX1-Y99S (g), MRGPRX1-F237A (h), MRGPRX1-L240S (i) and MRGPRX1-W241R (j).

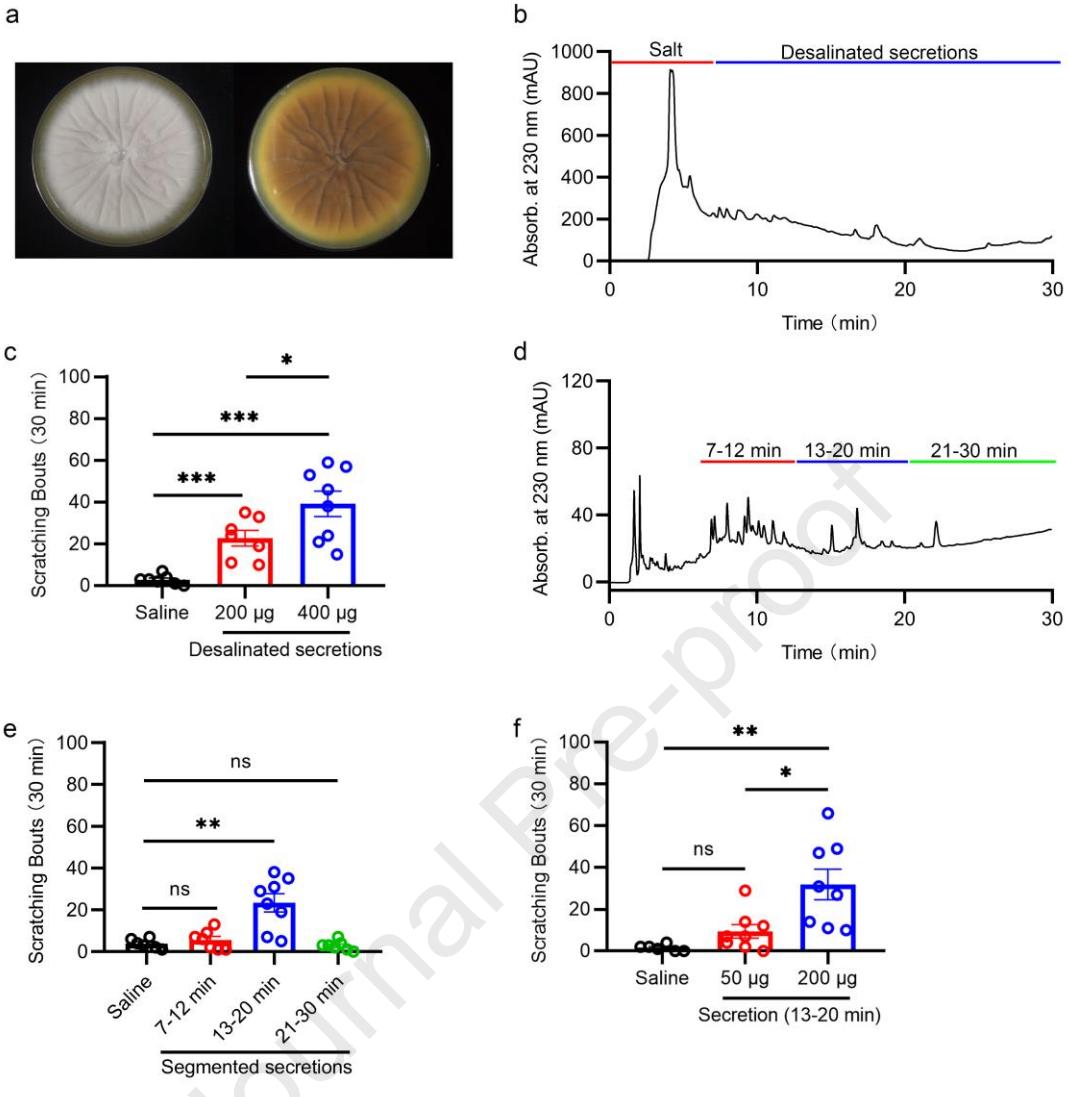

a

| Order | Accession | Description | Exp. q-value | Sum PEP Score | Coverage | # Peptides |
|---|---|---|---|---|---|---|
| 1 | XP_002844682.1 | extensin [*Microsporum canis* CBS 113480] | 0 | 57.18391673 | 34.47154472 | 11 |
| 2 | XP_002845450.1 | hsp70-like protein [*Microsporum canis* CBS 113480] | 0 | 43.63418916 | 11.62079511 | 8 |
| 3 | EEQ29258.1 | Cu, Zn superoxide dismutase [*Microsporum canis* CBS 113480] | 0 | 33.37843672 | 85.06493506 | 5 |
| 4 | 2LR5 | A Chain A, micasin | 0 | 27.94356862 | 100 | 3 |
| 5 | EEQ32886.1 | conserved hypothetical protein [*Microsporum canis* CBS 113480] | 0 | 25.9686595 | 52.05479452 | 8 |
| 6 | EEQ27779.1 | tenascin C [*Microsporum canis* CBS 113480] | 0 | 25.0766745 | 36.72654691 | 10 |
| 7 | XP_002849737.1 | antioxidant protein LsfA [*Microsporum canis* CBS 113480] | 0 | 24.58261093 | 16.28959276 | 6 |
| 8 | EEQ33402.1 | conserved hypothetical protein [*Microsporum canis* CBS 113480] | 0 | 21.29127406 | 16.30434783 | 3 |
| 9 | XP_002843445.1 | conserved hypothetical protein [*Microsporum canis* CBS 113480] | 0 | 16.27992768 | 22.68041237 | 4 |
| 10 | XP_002846678.1 | stress protein DDR48 [*Microsporum canis* CBS 113480] | 0 | 12.08446407 | 31.96480938 | 6 |